

## Multiple magnetic transitions in $\text{Er}_2\text{Ni}_2\text{Pb}$

Aravind D. Chinchure, E. Muñoz-Sandoval, and J. A. Mydosh

Kamerlingh Onnes Laboratory, Leiden University, 2300 RA Leiden, The Netherlands

(Received 9 March 2001; published 19 June 2001)

We have fabricated single-phase samples and measured the bulk properties for one (Er) of a series of ternary, heavy rare-earth, 221 ‘‘plumbide’’ intermetallic compounds  $R_2\text{Ni}_2\text{Pb}$  ( $R$  = rare earths). These materials form in the orthorhombic (space group  $Cmmm$ ) structure which is isostructural to  $\text{Mn}_2\text{AlB}_2$  compounds. Our results of susceptibility, magnetization, heat capacity, and (magneto) resistivity on  $\text{Er}_2\text{Ni}_2\text{Pb}$  show (sharp) multiple antiferromagnetic transitions and strong field dependences in all bulk properties for the temperature range 2–10 K. We relate this magnetic behavior to the unusual  $R$  symmetry (partially frustrated) of the highly anisotropic plumbide crystal structure.

DOI: 10.1103/PhysRevB.64.020404

PACS number(s): 75.30.-m, 75.40.Cx, 75.50.-y

New magnetic materials remain an important topic of present-day research, especially when unusual or multiple magnetic phase transitions occur.<sup>1,2</sup> Very recently, synthesis of a series of ternary compounds with composition  $R_2\text{Ni}_2\text{Pb}$  ( $R$  = Y, Sm, Gd, Tb, Dy, Ho, Er, Tm, Lu) crystallizing in an orthorhombic  $\text{Mn}_2\text{AlB}_2$ -type structure with  $Cmmm$  space group has been reported in the literature.<sup>3</sup> These plumbide 221 intermetallic compounds were shown to form via arc melting and appear as the majority phase after a proper heat treatment (600 °C for four weeks). X-ray diffraction was used to determine the crystal structure<sup>3</sup> (which we discuss below). However, none of their physical properties were reported. In this Rapid Communication, we present the results of our investigations of magnetic susceptibility, magnetization, heat capacity, resistivity, and magnetoresistance measurements on the  $\text{Er}_2\text{Ni}_2\text{Pb}$  compound.

Two batches of polycrystalline samples of  $\text{Er}_2\text{Ni}_2\text{Pb}$  were synthesized by arc melting the constituent elements in the desired ratio on a water cooled copper hearth under high-purity argon atmosphere. To ensure homogeneity, the alloy buttons were remelted several times. One batch of the arc melted samples was annealed in an evacuated quartz ampoule at 600 °C for four weeks. The samples were analyzed using electron-probe microanalysis (EPMA) which proved them to be single phase (second phases less than 2%) and to have the desired 2:2:1 stoichiometry (within 2% resolution). Powder x-ray-diffraction measurements established that the samples have an orthorhombic structure with lattice parameters  $a = 4.0080(7)$  Å,  $b = 13.8997(3)$  Å, and  $c = 3.6031(2)$  Å in agreement with Gulay *et al.*<sup>3</sup> Scanning electron microscope (SEM) photos on the polished sample show the formation of large grains with preferential orientations along particular directions (mainly  $b$  axis) and unpolished samples exhibit layers, and steps at the edges or surfaces. The magnetic susceptibility ( $\chi$ ) and magnetization ( $M$ ) was measured using a Quantum Design SQUID magnetic property measurement system while the resistivity ( $\rho$ ), magnetoresistance [ $\rho(H)$ ] and heat capacity ( $C_p$ ) were measured using Quantum Design physical property measurement system.

$\text{Er}_2\text{Ni}_2\text{Pb}$  adopts the  $\text{Mn}_2\text{AlB}_2$ -type structure ( $Cmmm$ ).<sup>3</sup> Figure 1 illustrates the crystal structure emphasizing the  $R$ -atoms positions and gives the unit cell. In this structure, all

Er atoms in the unit cell are crystallographically equivalent. The Er atoms form layers consisting of Ni centered trigonal  $[\text{NiEr}_6]$  prisms and Pb centered slightly distorted cubes  $[\text{PbEr}_8]$ . This structure can also be described as packing of the columns of the Er-centered distorted pentagonal  $[\text{ErNi}_6\text{Pb}_4]$  prisms along the  $c$  axis. One of the important features of this structure is the packing sequence of trigonal prisms, cubes, and pentagonal prisms. The interatomic distances between Er-Ni, Er-Pb are significantly shorter than the sum of the respective atomic radii (indicative of strong bond), whereas Er-Er distances are close to or longer than the sum of their atomic radii (weakly bonding).

dc magnetic susceptibility of  $\text{Er}_2\text{Ni}_2\text{Pb}$  has been measured in a field of 0.1 T in the temperature interval from 1.8 to 300 K. To show the low temperature data clearly, we have plotted in Fig. 2 the susceptibility in the temperature interval from 1.8 to 10 K. Between 3.5 and 3.2 K, the magnetic susceptibility remains suspiciously flat, below which it drops rapidly with a hump around 2.3 K. This behavior below 3.5 K suggests that  $\text{Er}_2\text{Ni}_2\text{Pb}$  undergoes multiple magnetic transitions (most probably antiferromagnetic in nature). The inset in Fig. 2 shows the inverse of susceptibility in the temperature range 1.8 to 300 K. The effective moment per Er ion obtained from a Curie-Weiss fit to the high temperature magnetic susceptibility is  $\mu_{\text{eff}} = 9.5 \mu_B$ . This value is close to the free ion moment of  $\text{Er}^{3+}$  ( $\mu_{\text{eff}} = 9.6 \mu_B$ ) which establishes that the Er ions are in the trivalent state and also suggests that Ni is not magnetic in this compound. A linear extrapo-

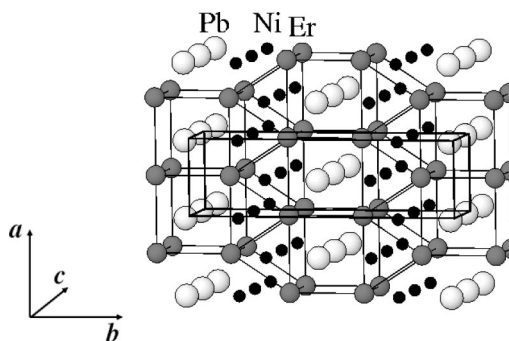


FIG. 1. Orthorhombic crystal structure ( $Cmmm$ ) of  $R_2\text{Ni}_2\text{Pb}$  with  $R = \text{Er}$ . The unit cell is indicated by the dark lines.

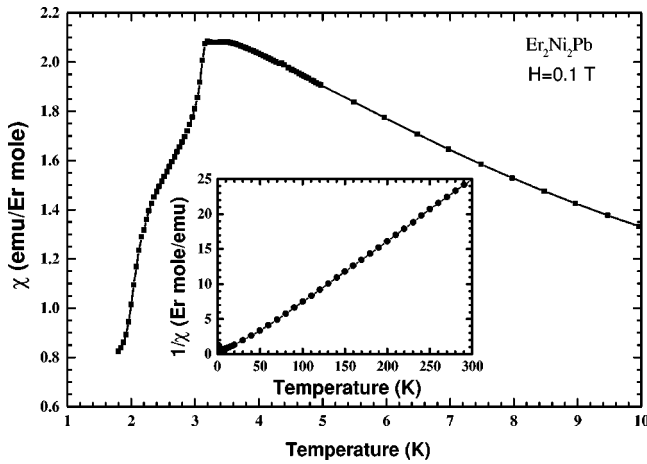


FIG. 2. dc-magnetic susceptibility of  $\text{Er}_2\text{Ni}_2\text{Pb}$  vs temperature. Inset: inverse susceptibility over the full temperature range.

lation of  $\chi^{-1}$  to  $T=0$  gives the Curie-Weiss paramagnetic temperature  $\Theta_p$ . Here  $\Theta_p = +15$  K, indicating a net ferromagnetic exchange coupling. Below 50 K, the susceptibility deviates from Curie-Weiss behavior to lower values due to the combined effects of crystal field and magnetic exchange interaction.

The temperature dependence of the electrical resistivity is presented in Fig. 3 for the temperature region between 1.8 and 10.0 K. The magnetic ordering is reflected by a sharp knee in the resistivity at 3.3 K and a smaller anomaly at 2.3 K. The temperatures of these anomalies are consistent with the magnetic susceptibility data. The inset of Fig. 3 plots the resistivity between 1.8 and 300 K. Above 4 K,  $\rho(T)$  shows typical, good metallic behavior with a nearly linear T coefficient.

Heat capacity ( $C_p$ ) of  $\text{Er}_2\text{Ni}_2\text{Pb}$  was measured in the temperature range of 1.8 to 25.0 K. In order to clearly see the low temperature data, we plot only the temperature range of 1.8 to 10.0 K as shown in Fig. 4. Two well-resolved close-by peaks at 3.4 and 3.2 K and a hump at 2.0 K are exhibited in the heat capacity. The temperatures at which the two peaks occur corresponds to the temperatures where the “flatness”

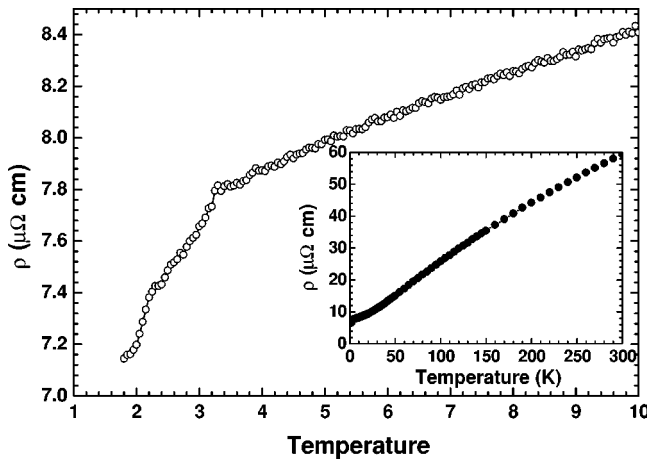


FIG. 3. Electrical resistivity vs temperature. Inset: resistivity over full temperature range.

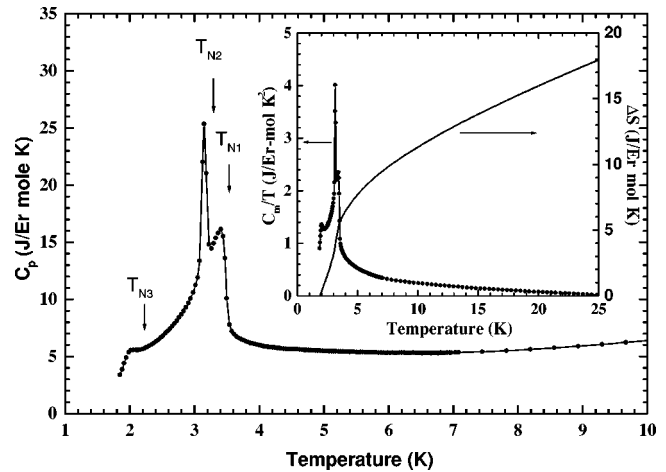


FIG. 4. Low temperature heat capacity of  $\text{Er}_2\text{Ni}_2\text{Pb}$  illustrating the three magnetic transitions. Inset: magnetic heat capacity divided by temperature and accumulated magnetic entropy vs temperature.

in the magnetic susceptibility begins and ends. The low-temperature anomaly in the heat capacity corresponds to the hump in the magnetic susceptibility. This confirms that the structures in the heat capacity at 3.4 K ( $T_{N1}$ ), 3.2 K ( $T_{N2}$ ) and 2.0 K ( $T_{N3}$ ) are due to complex and anisotropic magnetic ordering of  $\text{Er}^{3+}$  moments in  $\text{Er}_2\text{Ni}_2\text{Pb}$ .

In order to determine the magnetic contribution ( $C_m$ ) to the heat capacity, we subtracted the heat capacity of the non-magnetic allomorph  $\text{Y}_2\text{Ni}_2\text{Pb}$  assuming that the lattice contribution arising from phonon excitations, and electronic contribution originating from the conduction electrons and filled orbitals are the same in both the compounds. The inset of Fig. 4 shows the  $C_m/T$  vs  $T$  and its corresponding magnetic entropy in the temperature range of 1.8 to 25.0 K. The value of total entropy at 25 K is 18 J/Er mol K which is much smaller than the value  $R \ln 16 = R \ln(2J+1) \sim 23$  J/mol K, if the entropy would arise from the free ion ground state of  $J=15/2$  (16-fold degeneracy). This indicates the presence of strong crystal field effects. The entropy associated with the magnetic order is 6 J/Er mol K for  $\text{Er}_2\text{Ni}_2\text{Pb}$ . This value is close to that corresponding to a doublet ground state:  $R \ln 2 = 5.76$  J/Er mole K.

In order to obtain further understanding of the low temperature behavior of the magnetic susceptibility, resistivity, and heat capacity, we carried out isothermal magnetization measurements in an applied field ranging from 0 to 5 T and transverse magnetoresistance measurements in an applied field of 0 to 9 T. Figure 5 shows  $M$  vs  $H$  data of  $\text{Er}_2\text{Ni}_2\text{Pb}$  at 1.8 K, 2.5 K, and 5.0 K. In the ordered state, at 1.8 K, the behavior of magnetization ( $M$ ) keeps changing with applied field: (a) at first  $M$  is linear with field up to 0.2 T, (b) between 0.2 and 0.6 T,  $M$  rises steeply, (c) then shows a tendency to saturate between 0.6 and 1.0 T, (d)  $M$  again rises fast between 1.0 and 2.0 T, and finally (e) above 2.0 T,  $M$  saturate with saturation moment of  $9.0 \mu_B/\text{Er}$ . The steep rise in the  $M$  at two regions of applied field suggests two field-induced transitions in this compound before saturation above 2.0 T to its full free ion moment of  $9.0 \mu_B/\text{Er}$ . Similar behavior of magnetization was observed at 2.5 K with smaller

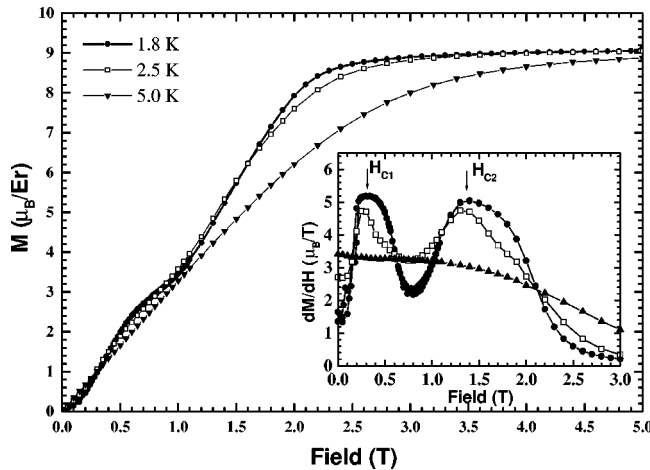


FIG. 5. Magnetization ( $M$ ) vs field ( $H$ ) at three temperatures. Inset:  $dM/dH$  vs  $H$  at the three temperatures. Note the two field induced transitions and the high field saturation.

effects compared to the magnetization behavior at 1.8 K. At 5 K,  $M$  initially varies linearly with magnetic field and then exhibits a tendency to saturate as is expected in the paramagnetic region.

The field dependence of isothermal, transverse ( $\vec{H} \perp \vec{I}$ ) magnetoresistance (MR),  $\Delta\rho/\rho = [\rho(H) - \rho(0)]/\rho(0)$ , where  $\rho(H)$  is the resistivity in magnetic field  $H$ , at 1.8 K, 3.0 K, and 5.0 K are plotted in Fig. 6. In the fully ordered state at 1.8 K, between 0 and 1.5 T, MR is positive and shows two peaks (of 3.5% and 2.5%) at 0.4 and 1.1 T. Above 1.5 T MR continues to decrease with a minimum (9.0%) around 2.6 T, it then starts increasing linearly with field up to 9.0 T and reaches a maximum value of 16.0%. At 3.0 K, the second peak in the MR disappears, the minimum in MR shifts to higher fields (3.0 T) with an increase in its value (15.0%), and a linear term for higher fields appear and changes its sign at 8.0 T. Above the magnetic orderings at 5.0 K, the two peaks in the MR disappear, however, the minimum in the MR still exists and increases linearly at higher fields without changing sign.

Careful observation of MR shows that the fields at which the two peaks in the magnetoresistance occur correspond to the fields where the peaks in the derivative of the magnetization with respect to field ( $dM/dH$ ) (see inset of Fig. 5) occur due to a metamagneticlike transition. The maximum (or peak) in the magnetoresistance can arise because of the two competing effects, (i) a positive contribution due to antiferromagnetic ordering, and (ii) a negative contribution from a ferromagnetic component which results from the metamagnetic transition.<sup>5</sup> Nevertheless, the increase of MR above 3 T causing a minimum in the magnetoresistance, the subsequent change of sign around 5.0 T and its high value of 16.0% at 9.0 T cannot be understood by traditional theories, such as Kohler's rule,<sup>4</sup> molecular field theory, and spin fluctuations.<sup>5</sup> Similar anomalous effects in the MR in completely different structures has also been observed in single crystalline  $\text{U}_2\text{Pt}_2\text{In}$  (fields up to 40 T),<sup>6</sup> and polycrystalline

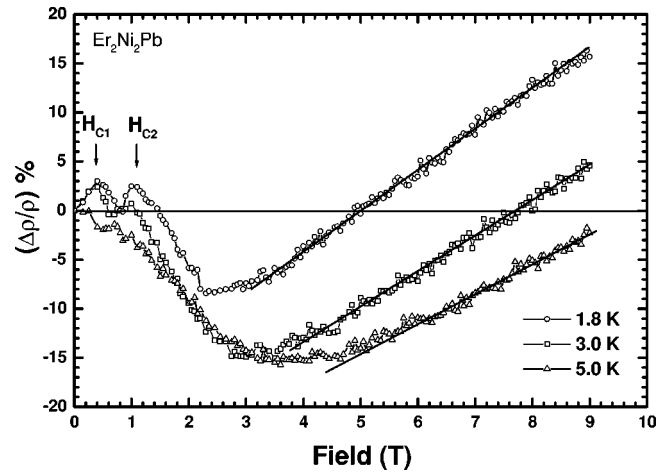


FIG. 6. Normalized (percent) change in the magnetoresistance vs field at three temperatures. Note the two field induced transitions and the linear behavior at high fields.

$\text{R}_2\text{Ni}_3\text{Si}_5$  ( $R$ =rare earths) (fields up to 4.5 T) where there are multiple transitions and a complicated magnetic ordering.<sup>7,8</sup>

Here we have presented our initial results of bulk measurements on polycrystal, single phase ( $\geq 98\%$ )  $\text{Er}_2\text{Ni}_2\text{Pb}$ . Based upon susceptibility, magnetization, heat capacity, and (magneto) resistivity data, this compound undergoes multiple (antiferro) magnetic transitions at 3.4 K and 3.2 K and 2.0 K. Field dependent magnetizations and magnetoresistance show the system to exhibit a series of metamagneticlike transitions below 2 K at 0.5 and 1.1 T. In addition, there are maximum/minimum and change of sign effects in the magnetoresistance at larger fields. These results point to a highly anisotropic magnetic behavior with unusual (or partially frustrated) spin structures. The origin of the multiple magnetic transitions in this material could be due to the existence of different magnetic exchange coupling between and within the Er planes in Ni centered trigonal  $[\text{NiEr}_6]$  prisms and Pb centered slightly distorted cubes  $[\text{PbEr}_8]$  (see Fig. 1). Thus, competing and frustrating magnetic interactions are present and will create complex magnetic transitions. The tendency of magnetization saturation in the paramagnetic region could be either due to the mixing of crystal field levels at higher fields or existence of magnetic correlations (precursor effects) above the magnetic ordering temperature.

In order to further probe this material (and other rare-earth compounds of the 221 symmetry), neutron powder diffraction is required to resolve the details of the magnetic structure. Also single crystals should be grown so that via different external fields orientations the magnetic anisotropy (hard/easy axes) can be determined. We are presently involved in such experiments.

We would like to acknowledge T.J. Gortemulder and R.W.A. Hendrikx for EPMA and x-ray analysis. E. Muñoz-Sandoval thanks the Consejo Nacional de Ciencia y Tecnología of Mexico (CONACyT) for financial support. This work was partially supported by the Dutch Foundation FOM.

- <sup>1</sup>See, for example, the series of articles in *Handbook of Magnetic Materials*, edited by K. H. J. Buschow (North Holland–Elsevier, Amsterdam, 1980–2000), Vols. 1–12.
- <sup>2</sup>See, Proceedings “44th Annual Conference on Magnetism and Magnetic Material” [J. Appl. Phys. **87**, 4653–5892 (2000)].
- <sup>3</sup>L. D. Gulay, Ya. M. Kalychak, and M. Wolcyrz, J. Alloys Compd. **311**, 228 (2000).
- <sup>4</sup>J. M. Ziman, *Electrons and Phonons* (Oxford University Press, London, 1963), p. 490; A. A. Abrikosov, *Fundamentals of the Theory of Metals* (North Holland–Elsevier, Amsterdam, 1988), p. 83; Robert C. O’Handley, *Modern Magnetic Materials: Principles and Applications* (Wiley, New York, 2000), p. 568.
- <sup>5</sup>Hiroshi Yamada and Satoshi Takada, J. Phys. Soc. Jpn. **34**, 51 (1973); Prog. Theor. Phys. **48**, 1828 (1972).
- <sup>6</sup>P. Estrela, Ph.D. thesis, University of Amsterdam, The Netherlands, 2000.
- <sup>7</sup>Chandam Mazumdar, K. Ghosh, R. Nagarajan, S. Ramakrishnan, B. D. Padalia, and L. C. Gupta, Phys. Rev. B **59**, 4215 (1999).
- <sup>8</sup>Chandam Mazumdar, A. K. Nigam, R. Nagarajan, L. C. Gupta, C. Godart, B. D. Padalia, G. Chandra, and R. Vijayraghavan, Phys. Rev. B **54**, 6069 (1996).